

STABLE HIGH CONDUCTIVITY BILAYERED ELECTROLYTES FOR LOW TEMPERATURE SOLID OXIDE FUEL CELLS

Eric D. Wachsman

**Department of Materials Science and Engineering
University of Florida
Gainesville, Fl, 32611**

[S. Boyapati M. Camaratta K. Duncan A. Jaiswal S.-H. Jung J.-Y. Park N. Jiang (SRI)]

Department of Energy, Contract Number: DE-AC26-99FT40712

WHY LOW TEMPERATURE (< 600 °C)?

Metallic Interconnects

Lower cost and greater reliability

Easier Sealing

Lower cost and greater reliability

Smaller Thermal Mismatch

Greater reliability → Lower cost

Less Insulation

Lower cost

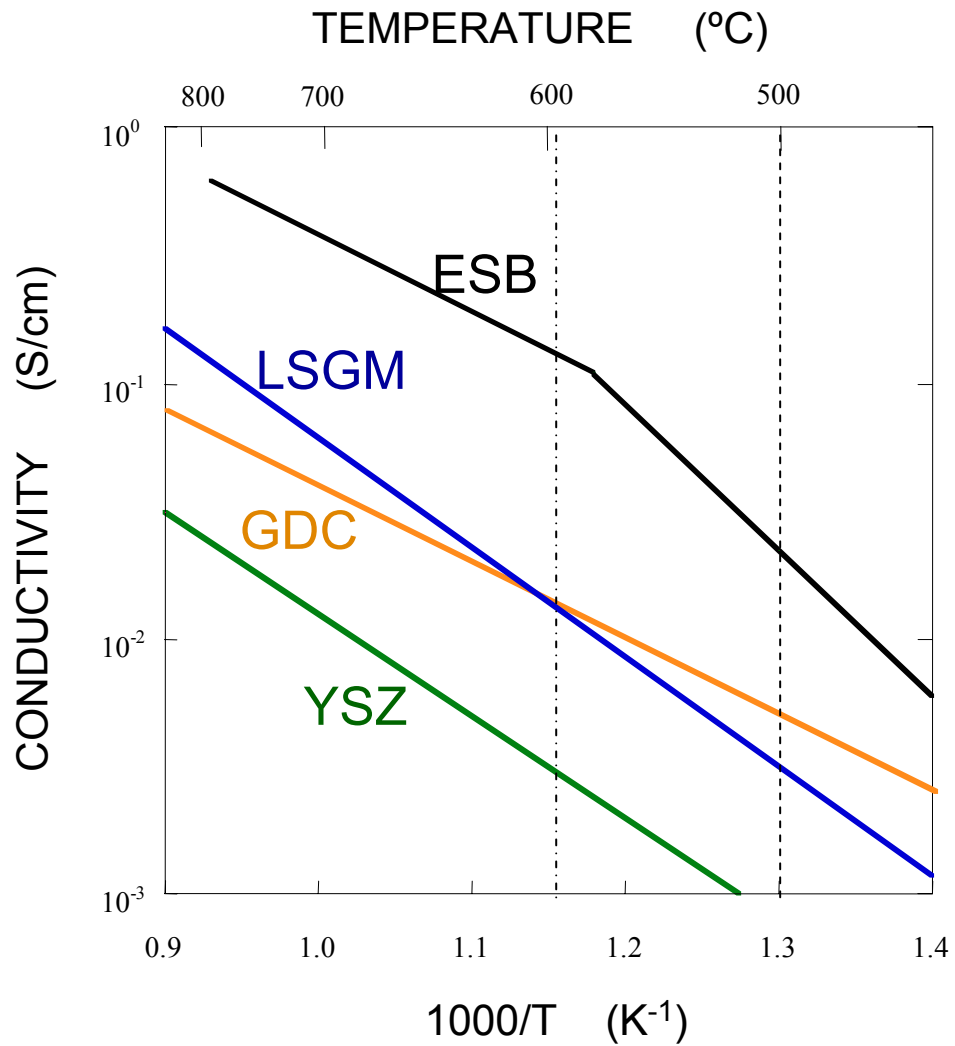
Rapid Startup with Less Energy Consumption

Lower cost and better performance

Stable High Surface-Area Electrodes

Better performance → Lower cost

CONDUCTIVITY OF VARIOUS ELECTROLYTES



Ceria-Conductivity & Bismuth Oxide-Structure in Reducing Conditions

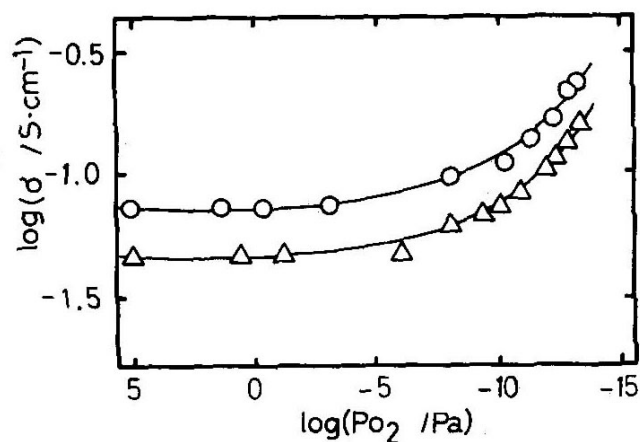


Fig. 6. Electrical conductivities as a function of oxygen partial pressure at 800°C: (O) $(\text{CeO}_2)_{0.8}(\text{SmO}_{1.5})_{0.2}$; (Δ) $(\text{CeO}_2)_{0.8}(\text{GdO}_{1.5})_{0.2}$.

Eguchi, et al., *Solid State Ionics*, **52**, 168 (1992)

Wachsman, et al., *Solid State Ionics*, **52**, 216 (1992)

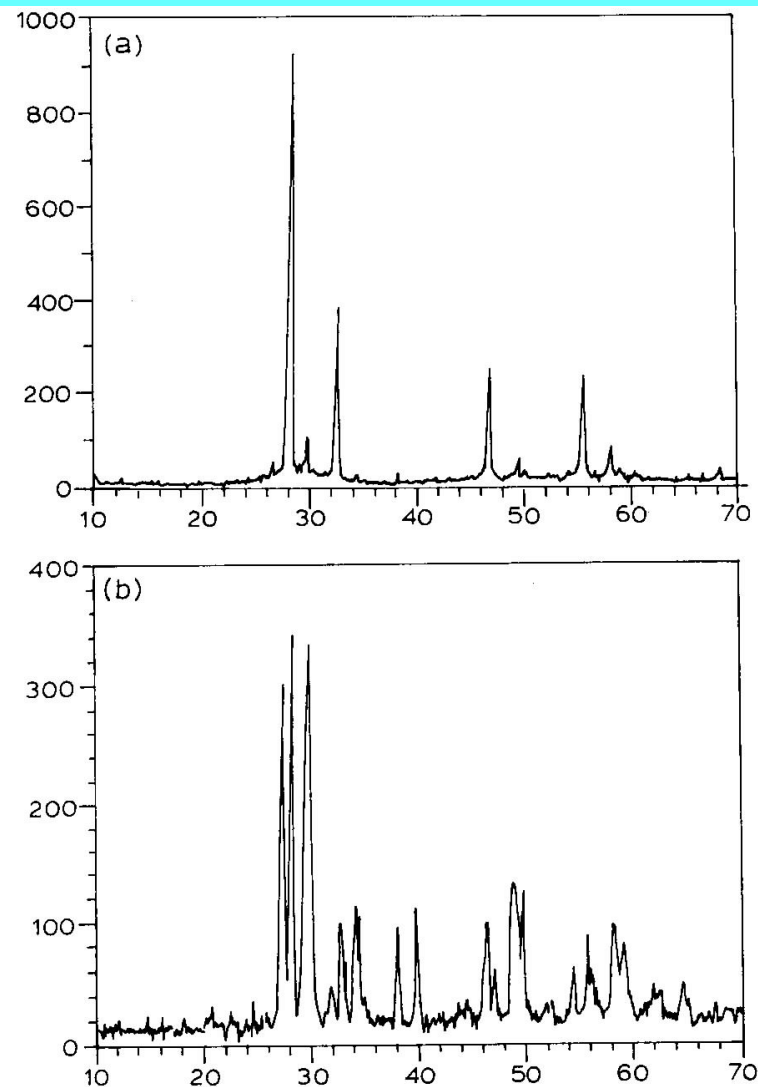
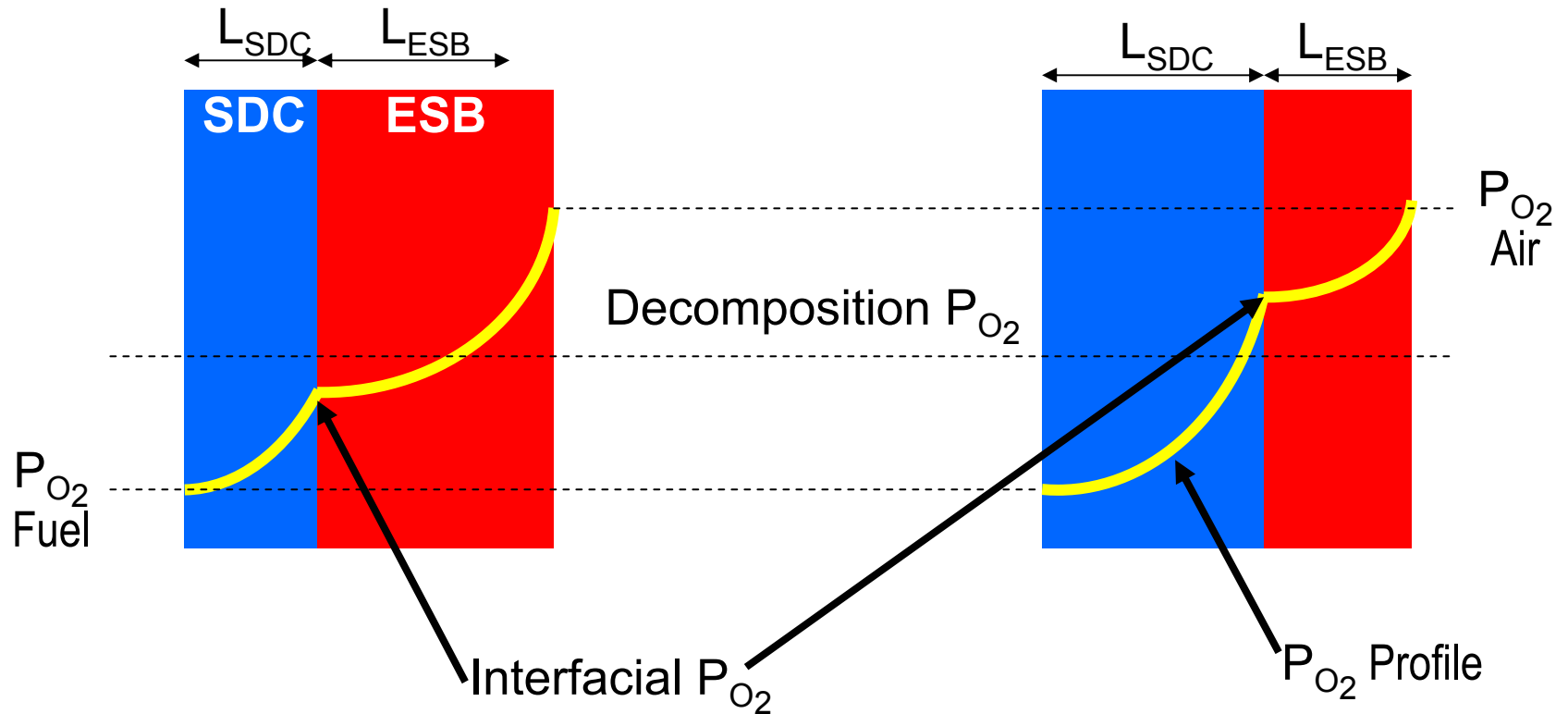


Fig. 4. X-ray diffraction of 20 mol% ESB: (a) as received; (b) annealed 4 h at 700 °C in $\text{H}_2/\text{H}_2\text{O}$ $P_{\text{O}_2} = 10^{-21}$ atm).

BILAYER CONCEPT



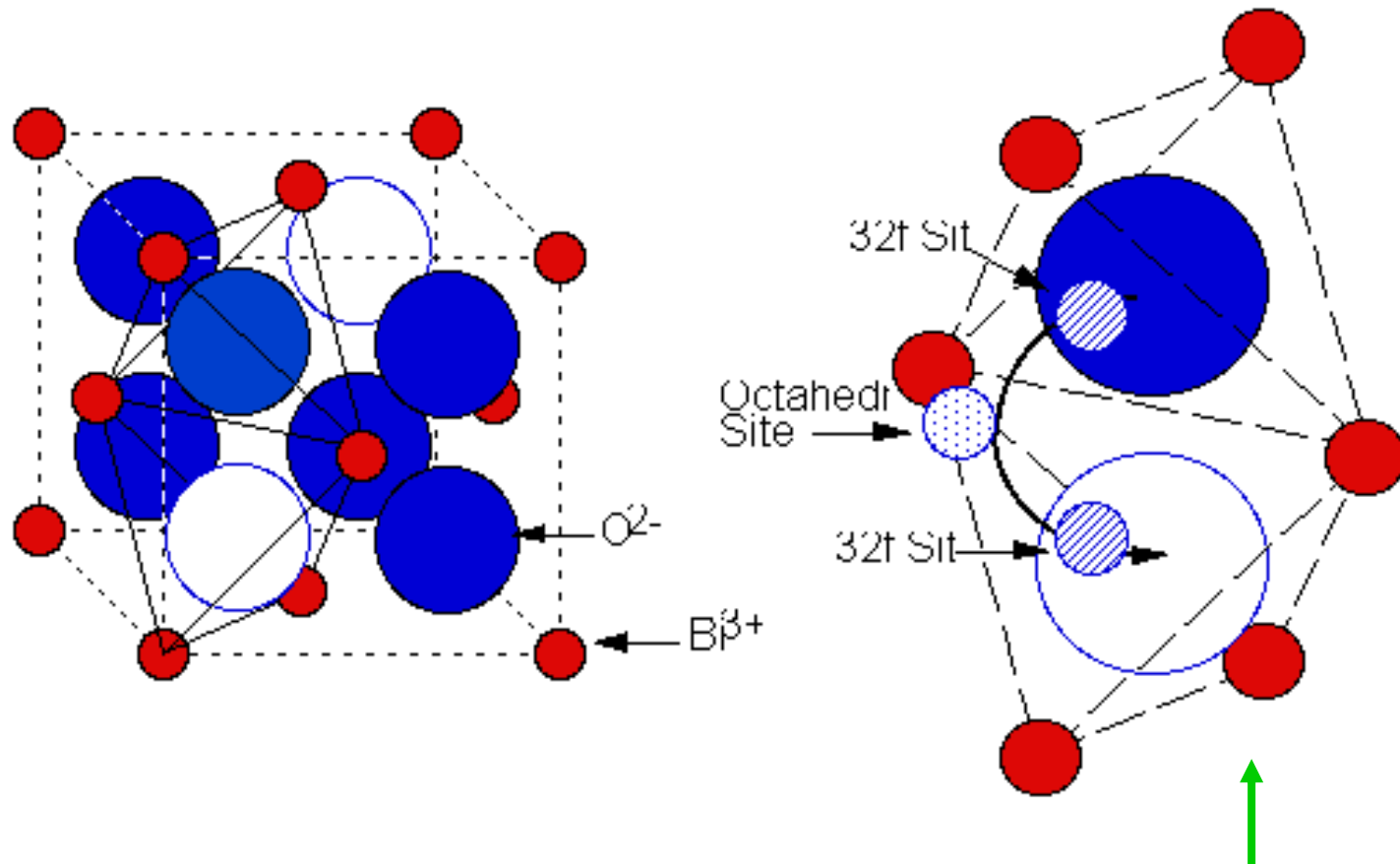
$$L_{SDC} / L_{ESB} < \tau_{optimal}$$

ESB decomposes

$$L_{SDC} / L_{ESB} > \tau_{optimal}$$

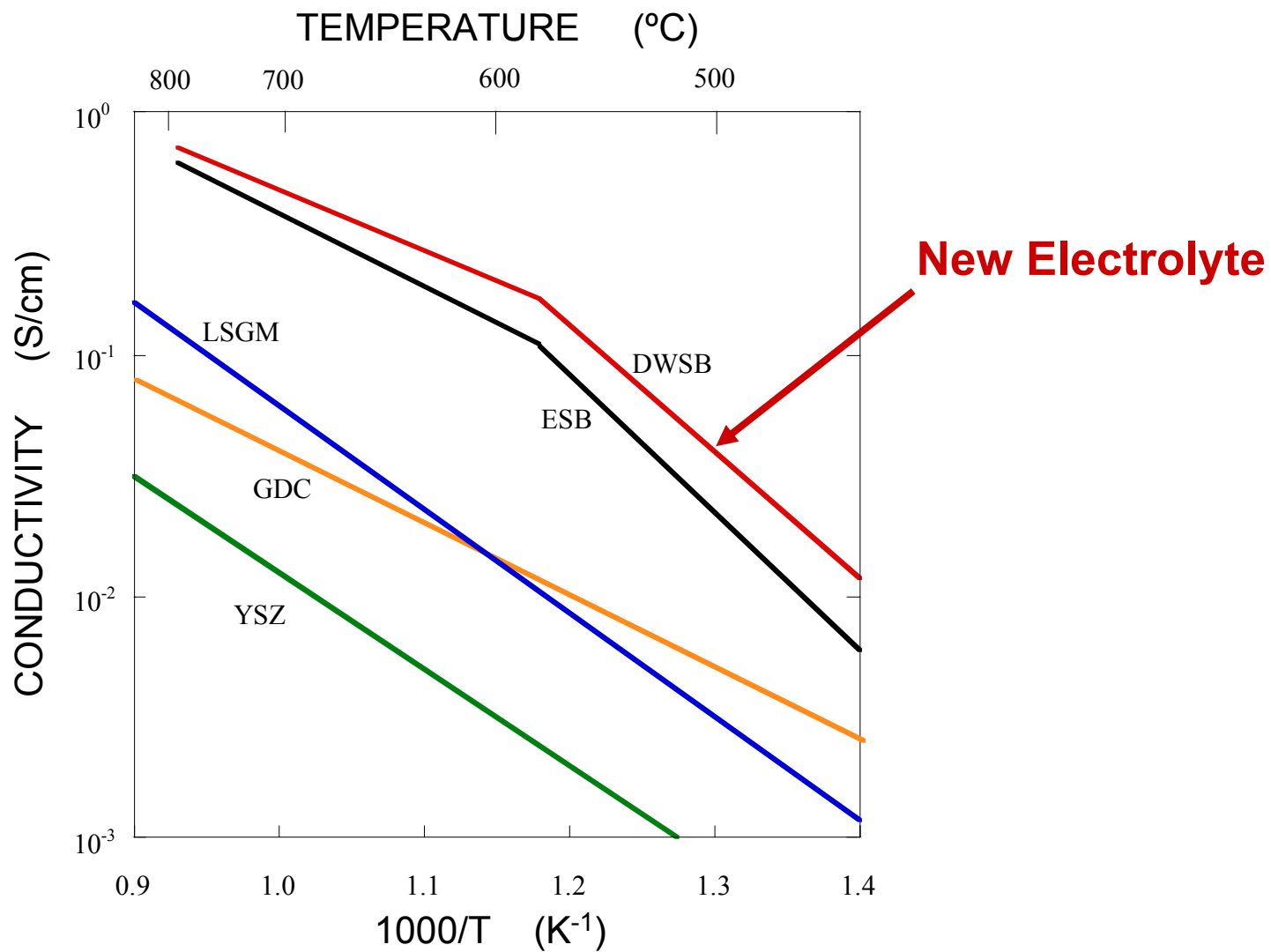
ESB is stable

FUNDAMENTALS OF IONIC TRANSPORT IN FLUORITE OXIDES



Jump from one tetrahedron to an adjacent tetrahedron in $\langle 100 \rangle$ direction

CONDUCTIVITY OF VARIOUS ELECTROLYTES



CONDUCTIVITY OF VARIOUS ELECTROLYTES @ 500 °C

Electrolyte	Conductivity (S/cm)	ASR ($\Omega\cdot\text{cm}^2$) 100 μm thick	ASR ($\Omega\cdot\text{cm}^2$) 10 μm thick
YSZ	0.00046	21.74	2.17
LSGM	0.0051	1.96	0.20
GDC	0.0095	1.05	0.11
ESB	0.021	0.48	0.05
DWSB	0.043	0.23	0.02

PULSED-LASER DEPOSITION: PROCEDURE & CHARACTERIZATION

1. *Pellet Preparation*

- Solid State Synthesis

2. *Preparation of Thin Films*

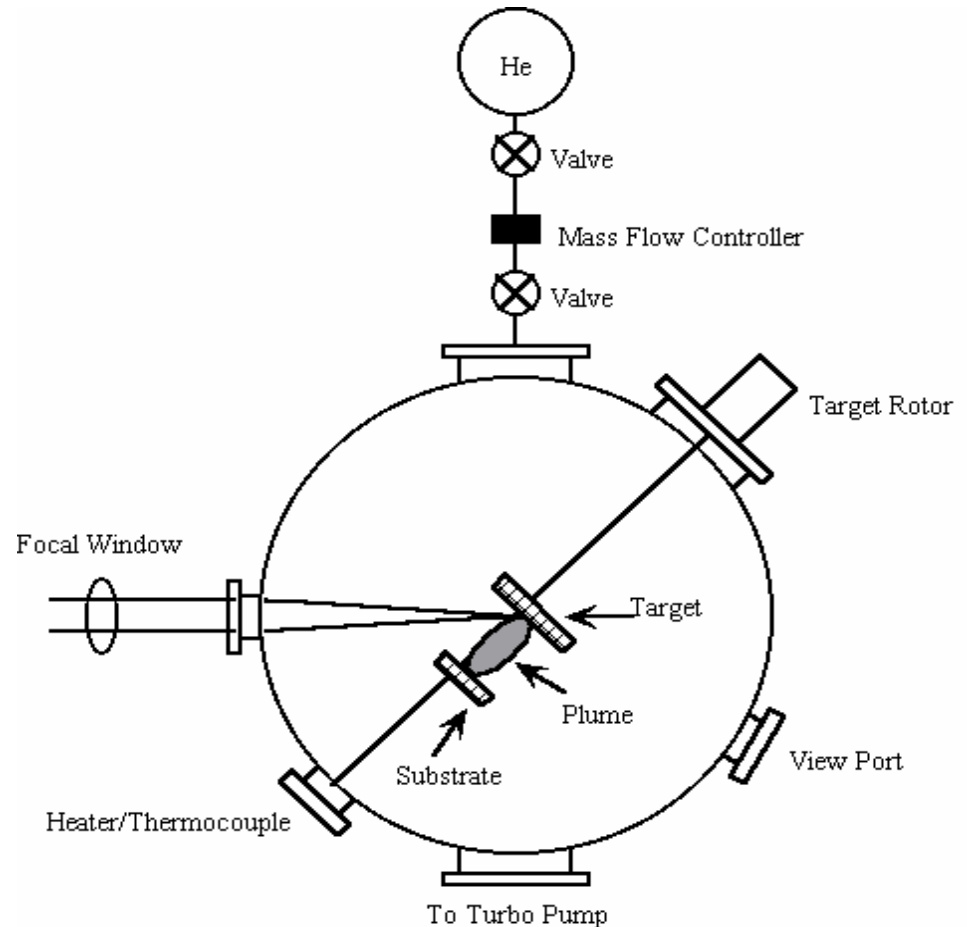
- Pulsed Laser Deposition (PLD)
- target: ESB, substrate: SDC

3. *Microstructural Analysis*

- Profilometry
- XRD, SEM, and EDS

4. *Electrical Measurement*

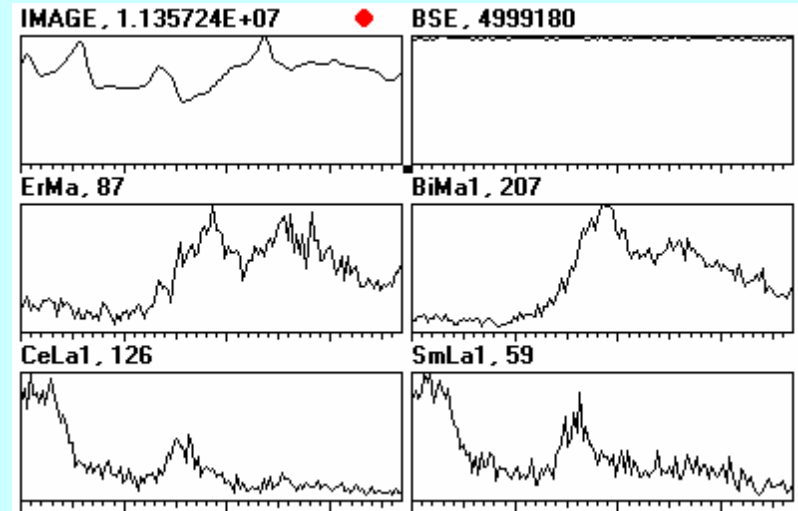
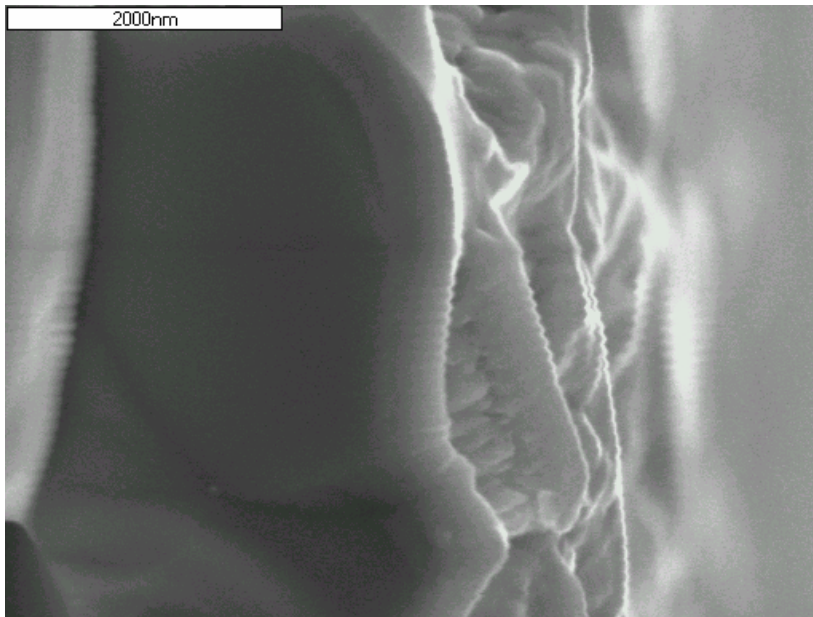
- AC Impedance Spectroscopy
(0.1 - 10MHz: 300 - 800°C)



PLD Operation

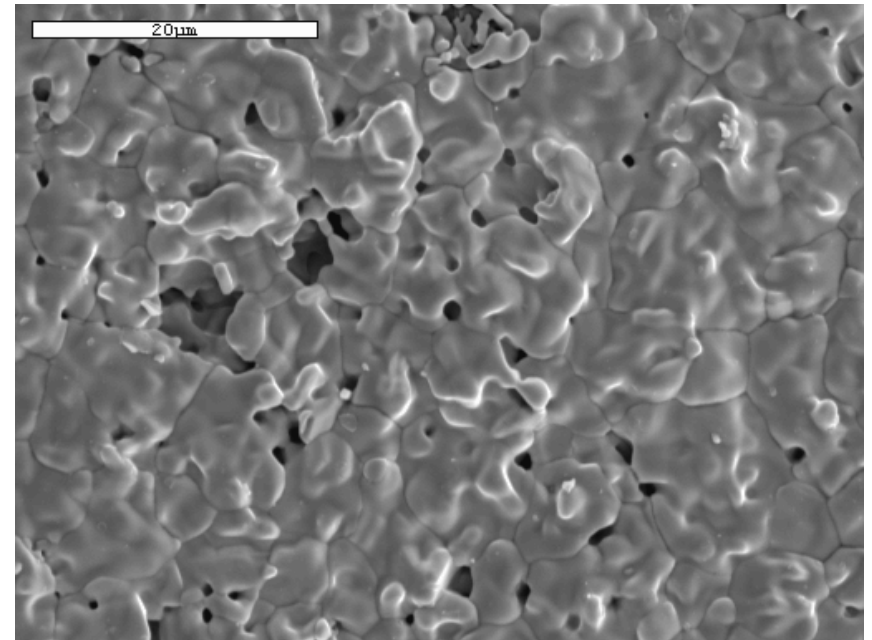
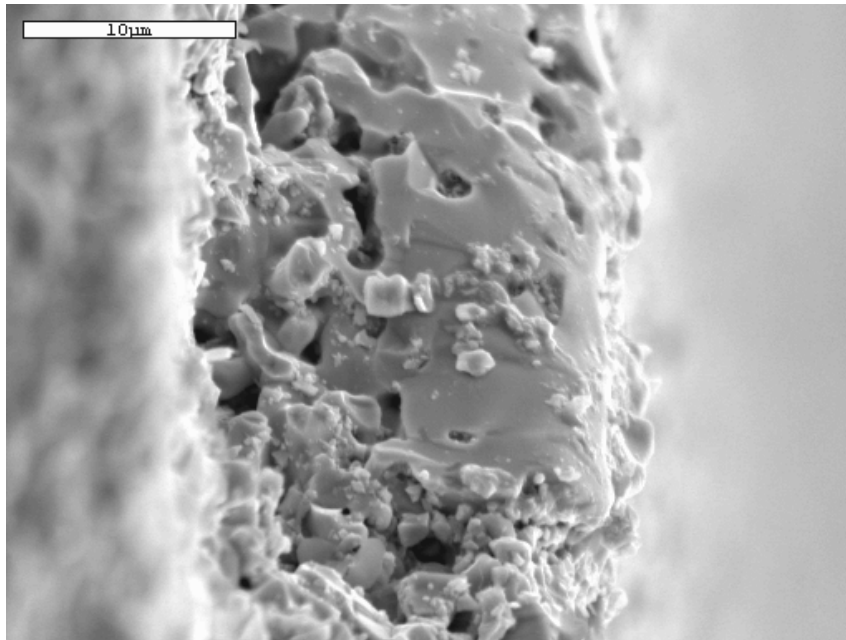
Characterization: SDC/ESB bilayer via Pulse-Laser Deposition (PLD)

Cross-section SEM micrograph
of SDC/ESB bilayer



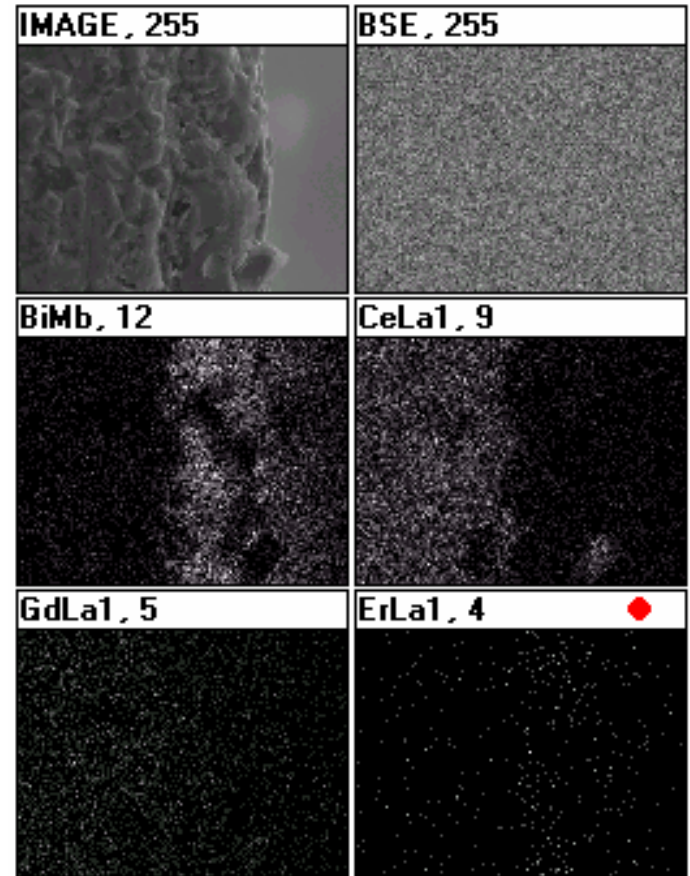
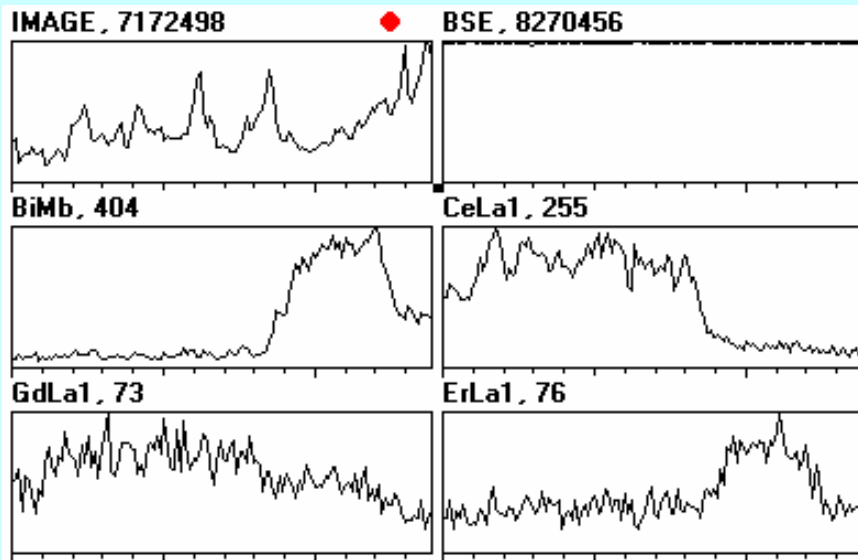
Chemical composition of
ESB/SDC bilayer from EDS
by X-ray linescan

Characterization: SDC/ESB bilayer via Dip-Coating



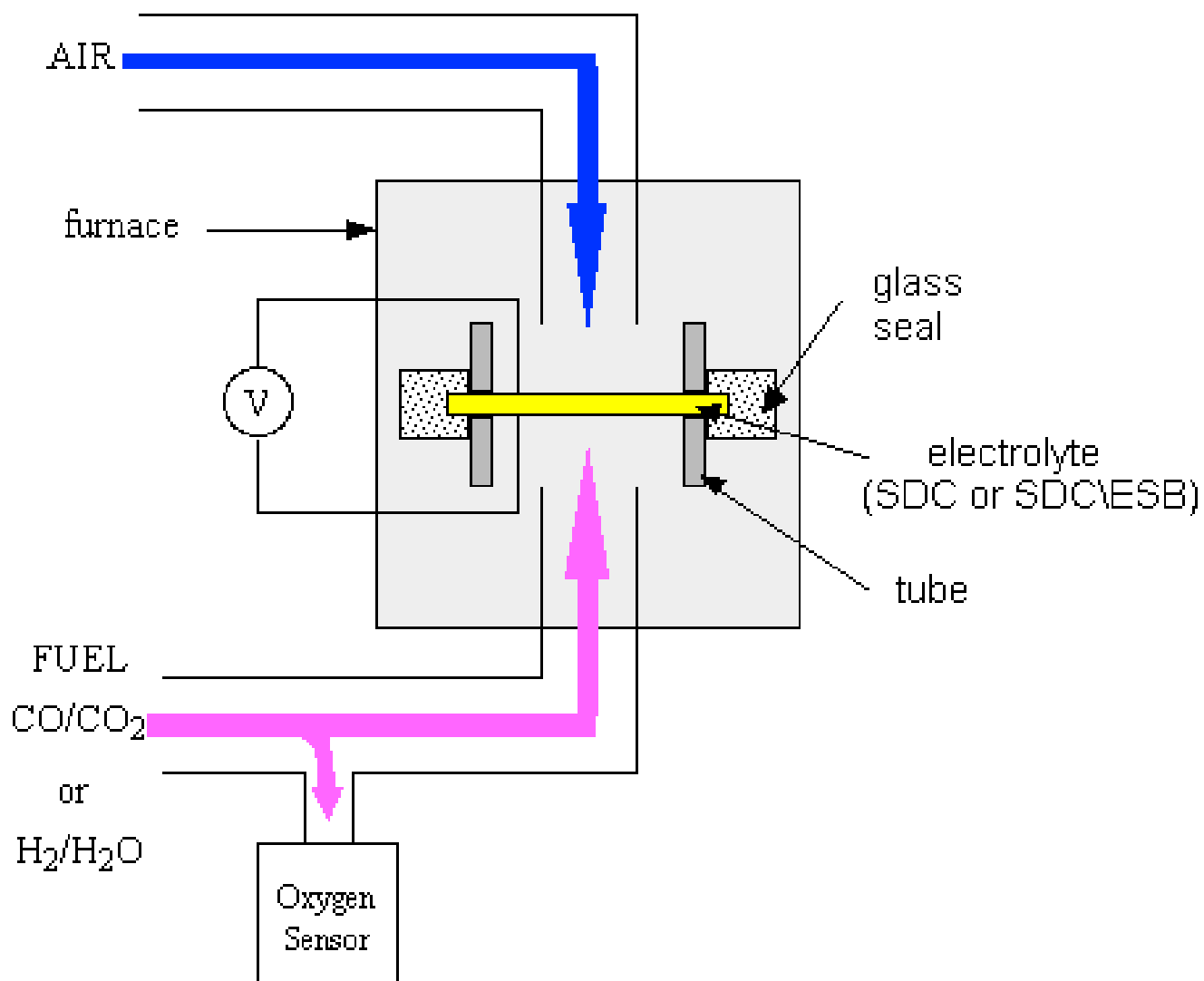
Cross-section and Surface
SEM micrograph of SDC/ESB bilayer

Characterization: SDC/ESB Bilayer via Dip-Coating

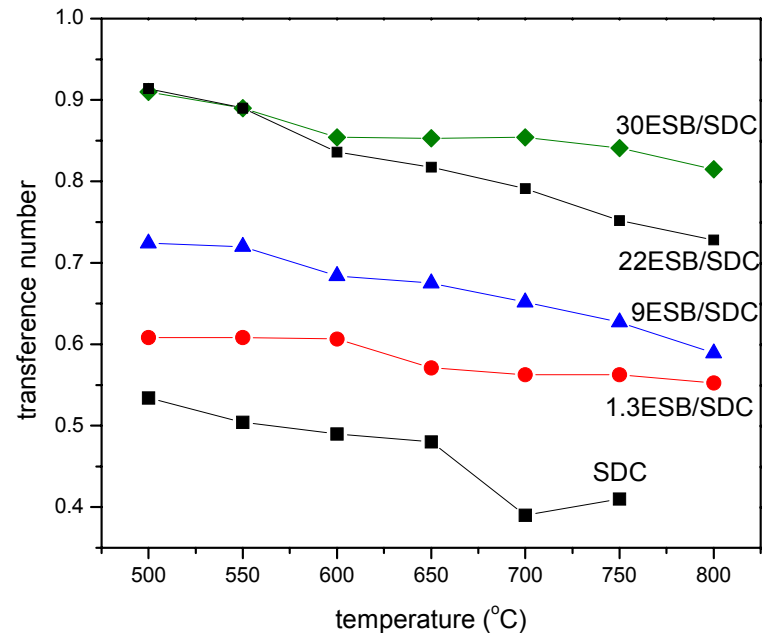
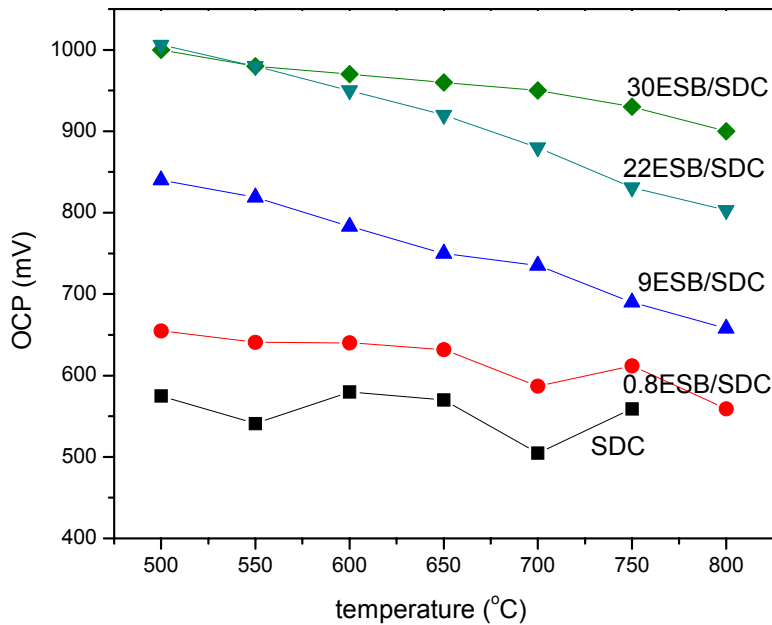


Chemical composition of ESB/SDC bilayer from EDS by X-ray linescan.....and mapping

FUEL CELL TESTING: SCHEMATIC

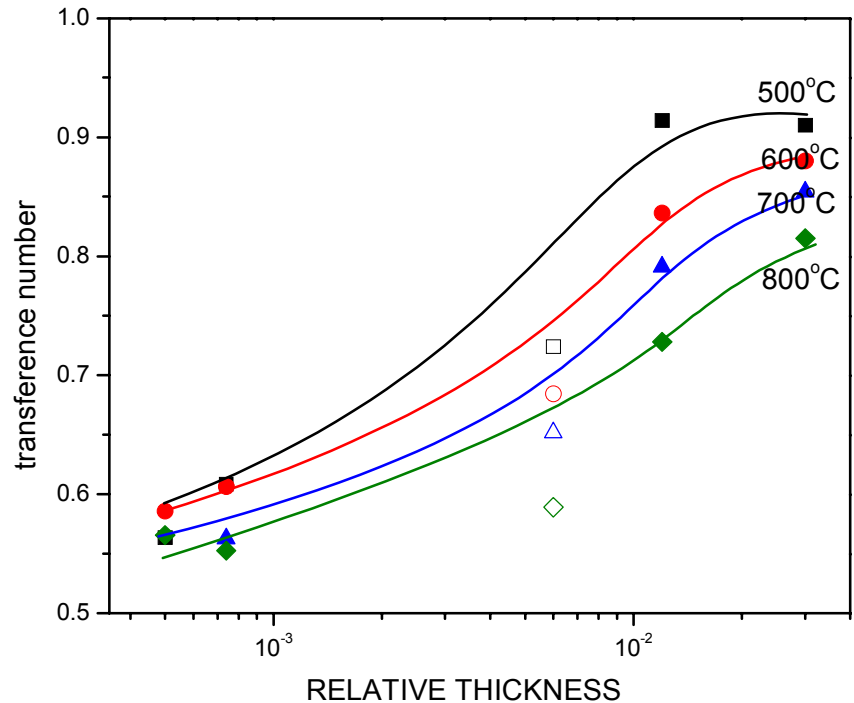
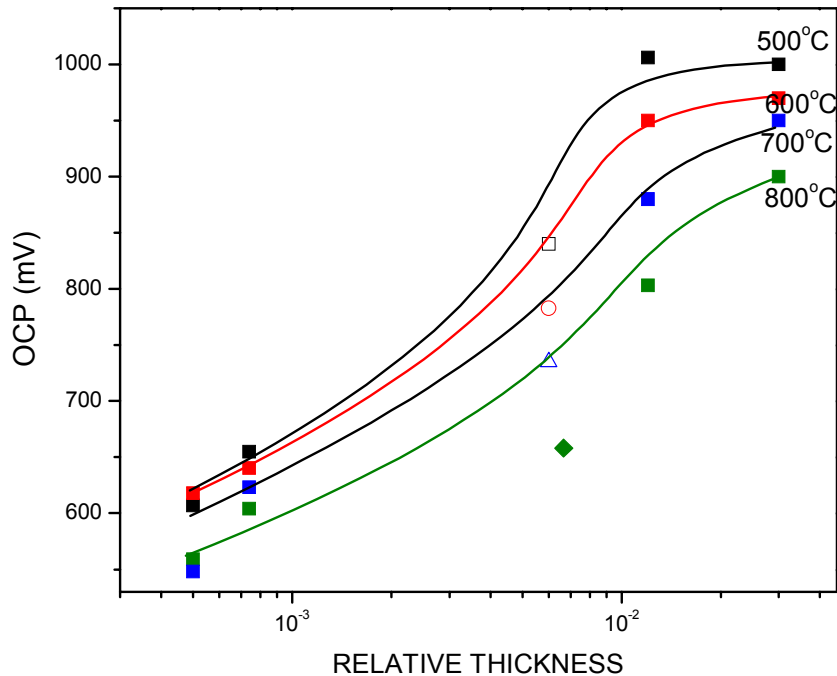


Characterization: OCP and t_i vs. Temperature for SDC and ESB/SDC Electrolytes



X ESB/SDC \equiv X μ m thick ESB layer on ~ 1.5 mm thick SDC substrate

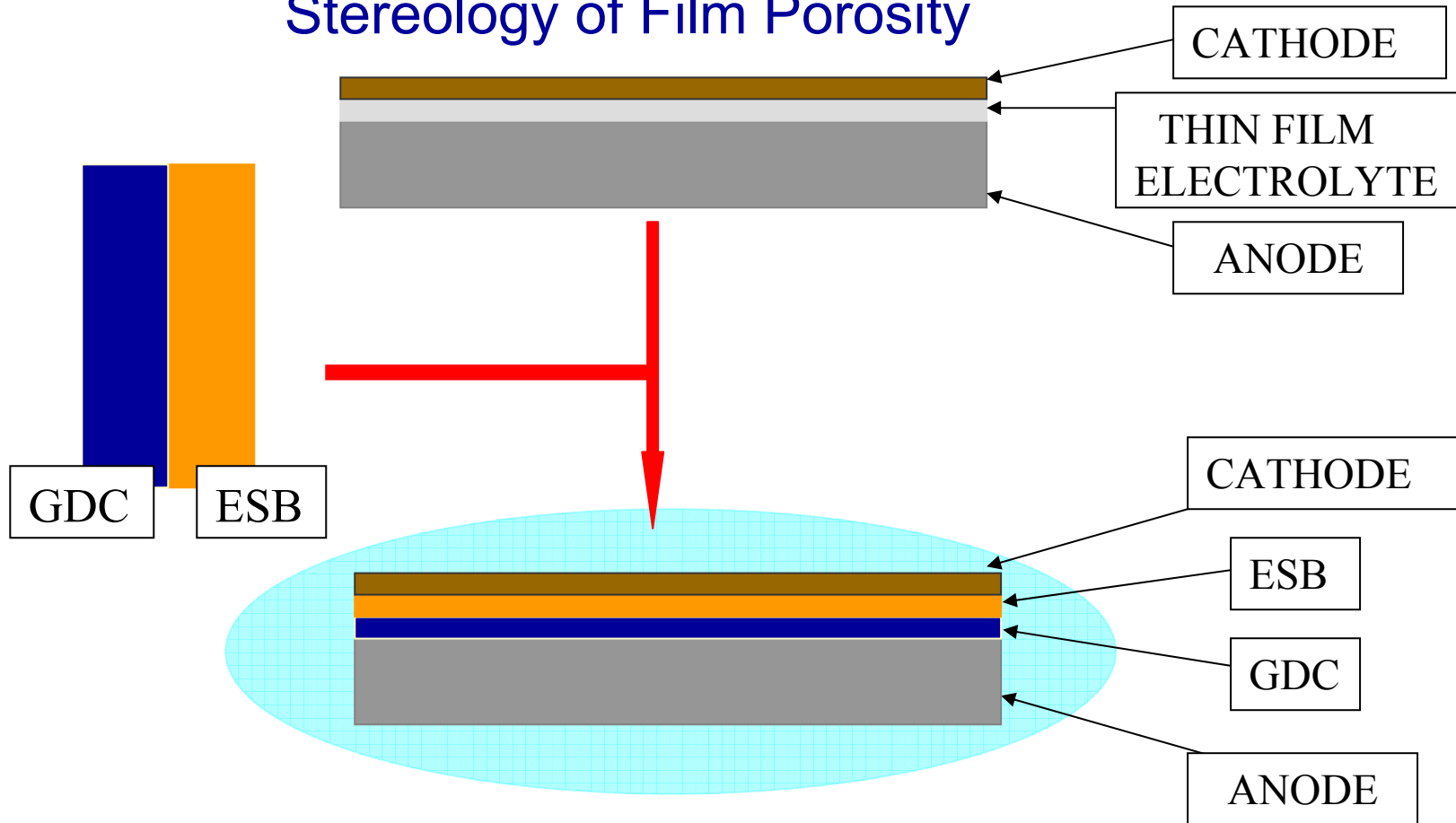
Effect of Relative Thickness on OCP & t_i for ESB/SDC Bilayer-Electrolyte SOFC with Air at the Cathode and H_2/H_2O at the Anode



Effect of ESB/SDC *relative thickness* on (a) *open-circuit potential* and (b) *transference number* of bilayer electrolyte SOFC with air on the cathode side and H_2/H_2O on the anode side (open symbols: data obtained with a porous ESB film).

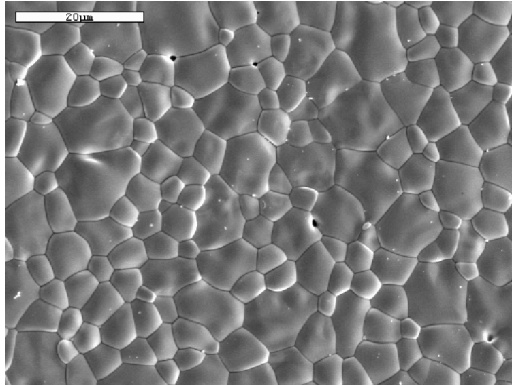
Electrode supported thin-film electrolyte systems Quantitative

Stereology of Film Porosity



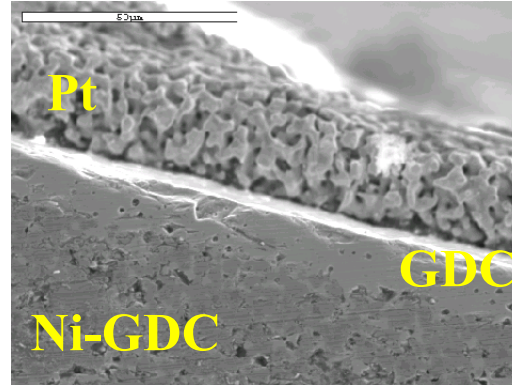
Thick Film GDC Electrolyte by Colloidal Deposition on Porous Ni-GDC Cermet

Surface



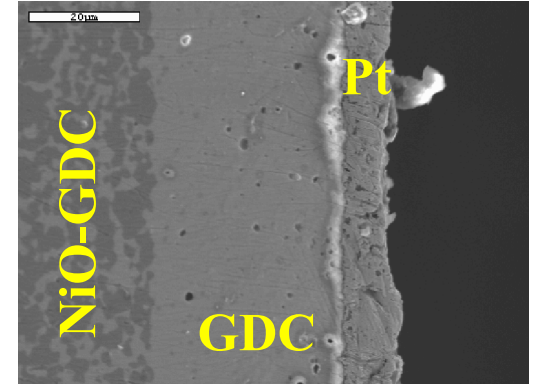
20μm

Cross-section 5coats



50μm

Cross-section 15coats



20μm

Sintering Conditions

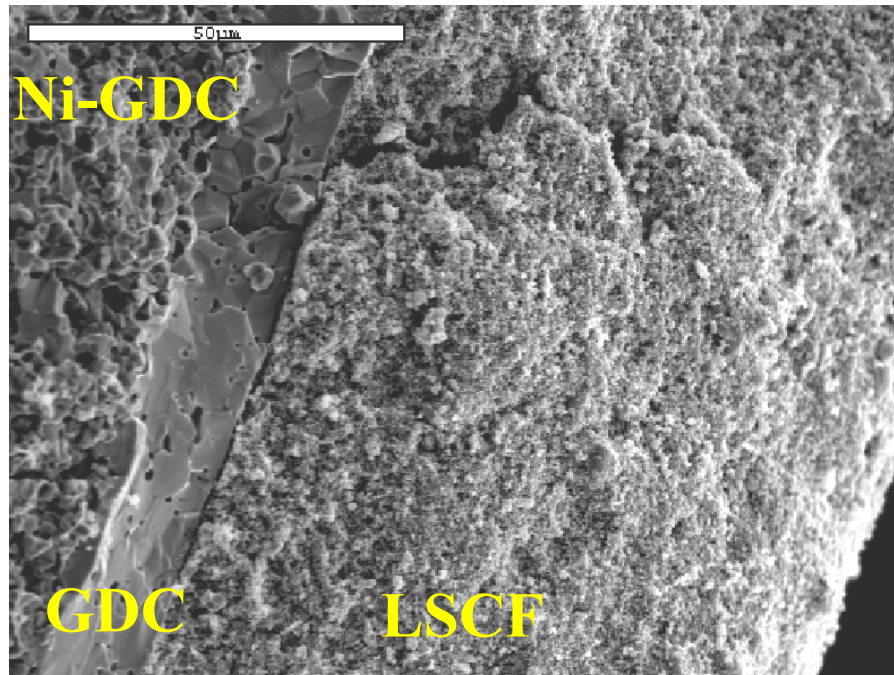


Pre-sintering: 850°C/4hrs

Final sintering: 1600°C/6hrs

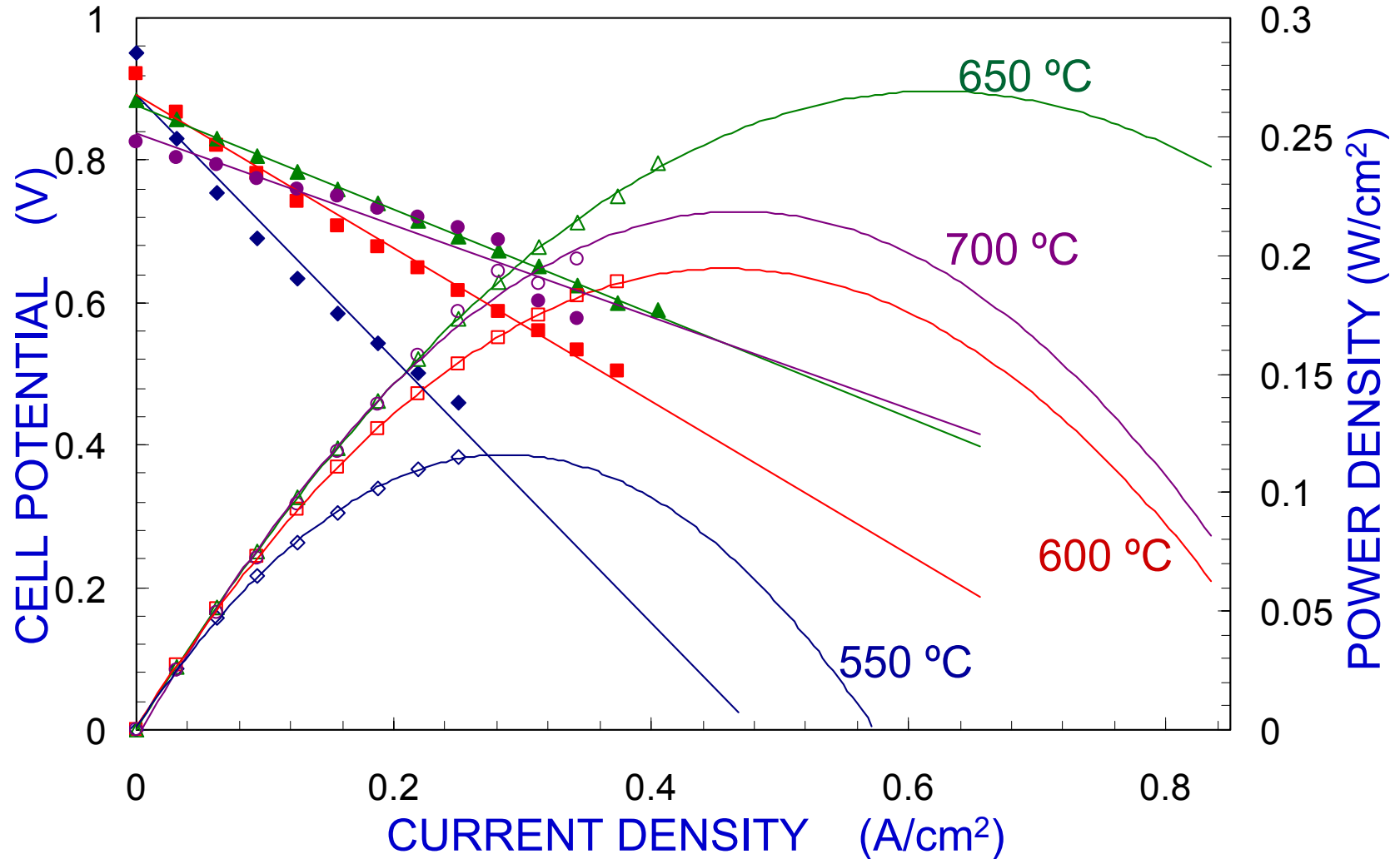
Fractured Section of Fuel Cell

Ni-GDC / GDC($\approx 15\mu\text{m}$) / LSCF($\approx 85\mu\text{m}$)

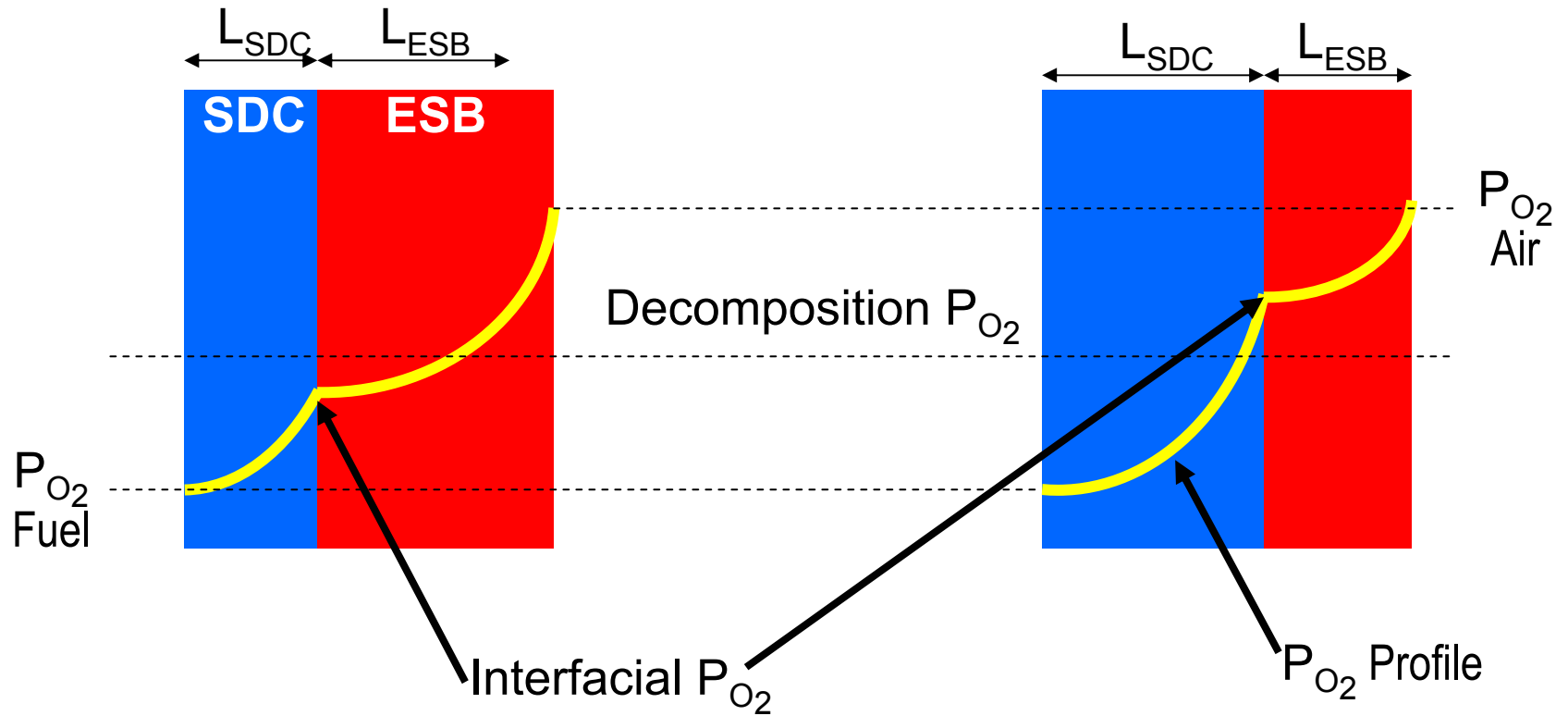


SOFC PERFORMANCE

H₂/H₂O, GDC-Ni / GDC / LSCF, Air



BILAYER CONCEPT



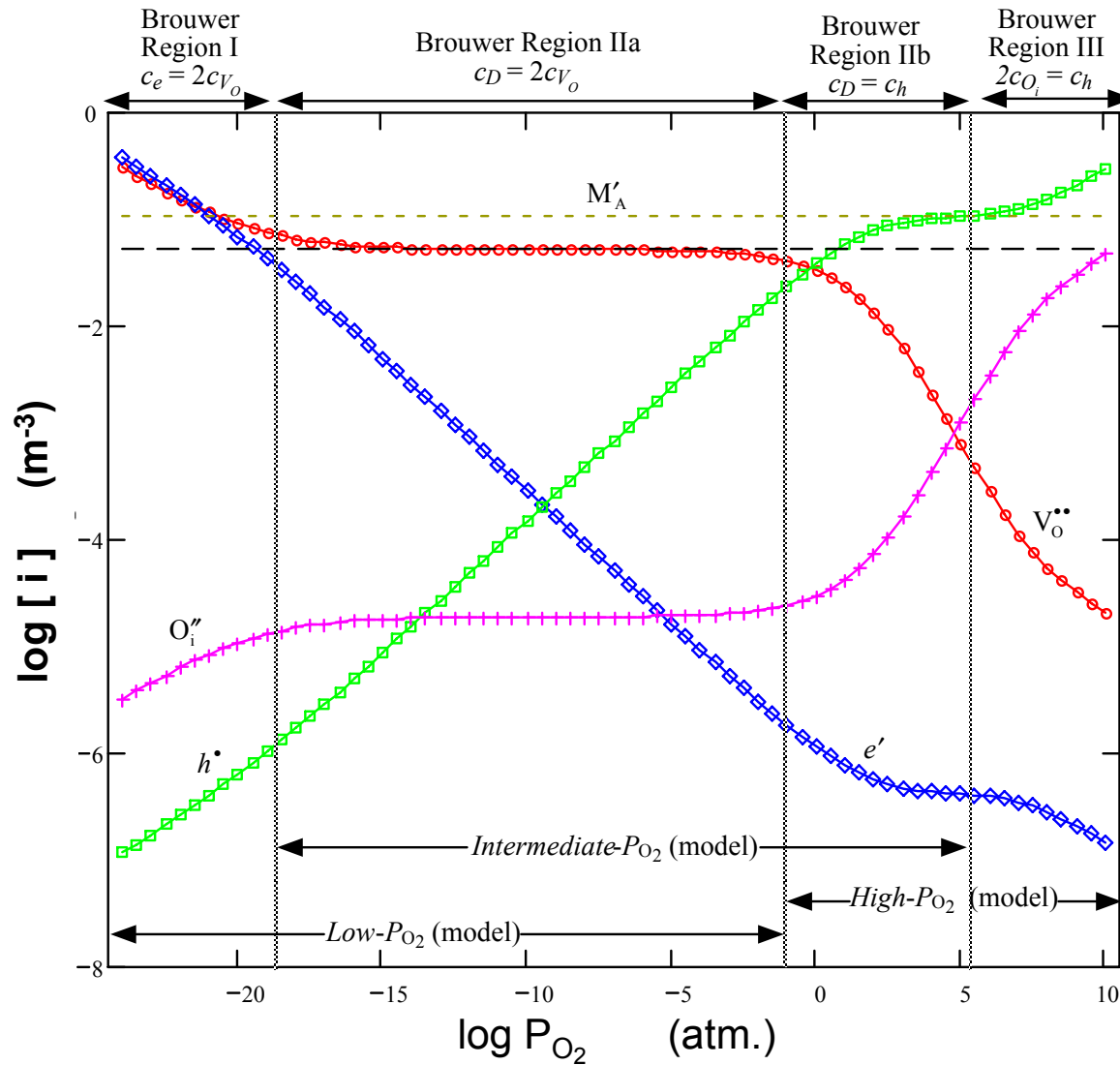
$$L_{SDC} / L_{ESB} < \tau_{optimal}$$

ESB decomposes

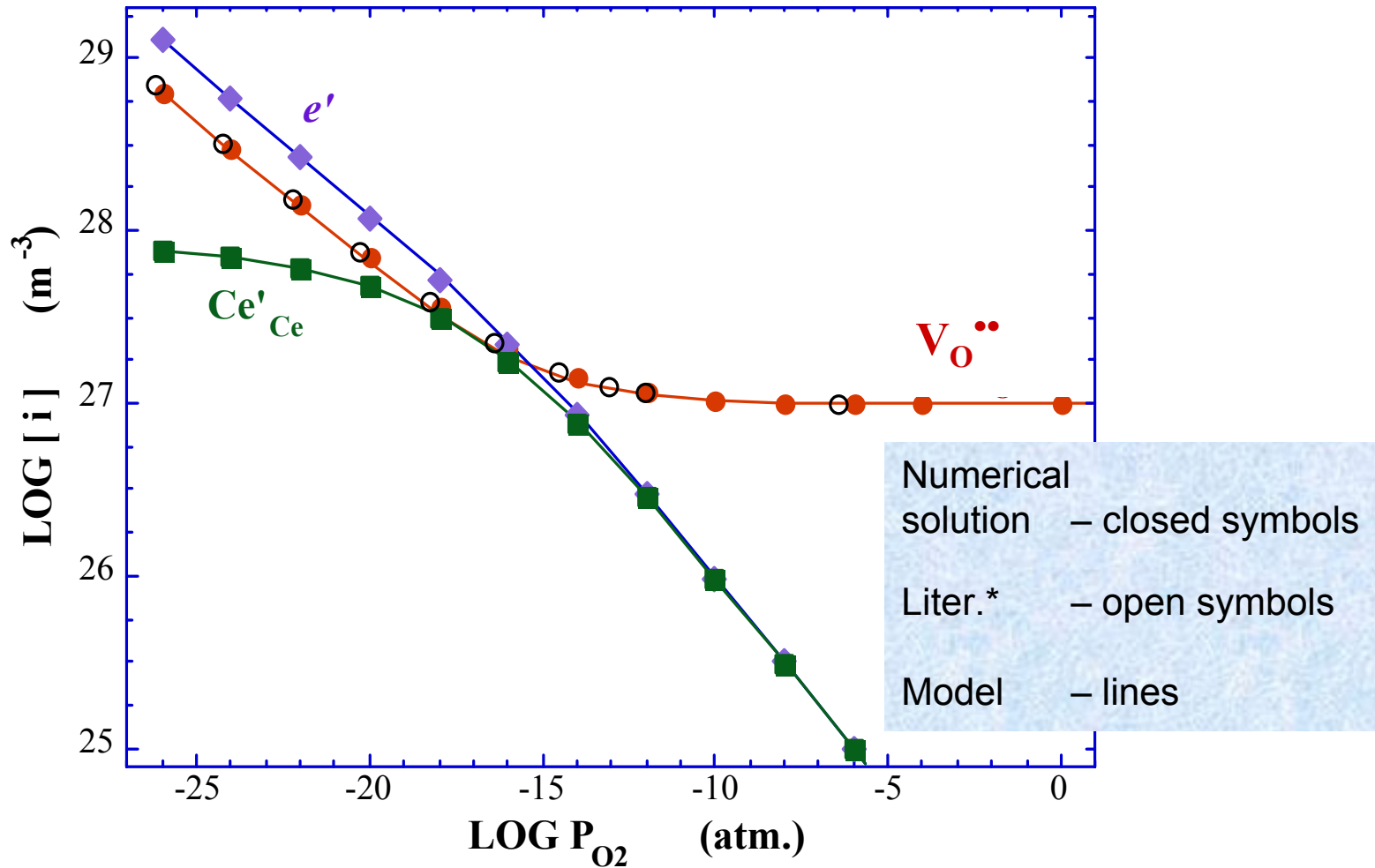
$$L_{SDC} / L_{ESB} > \tau_{optimal}$$

ESB is stable

MODELED DEFECT EQUILIBRIUM DIAGRAM FOR A FLUORITE-STRUCTURED OXIDE

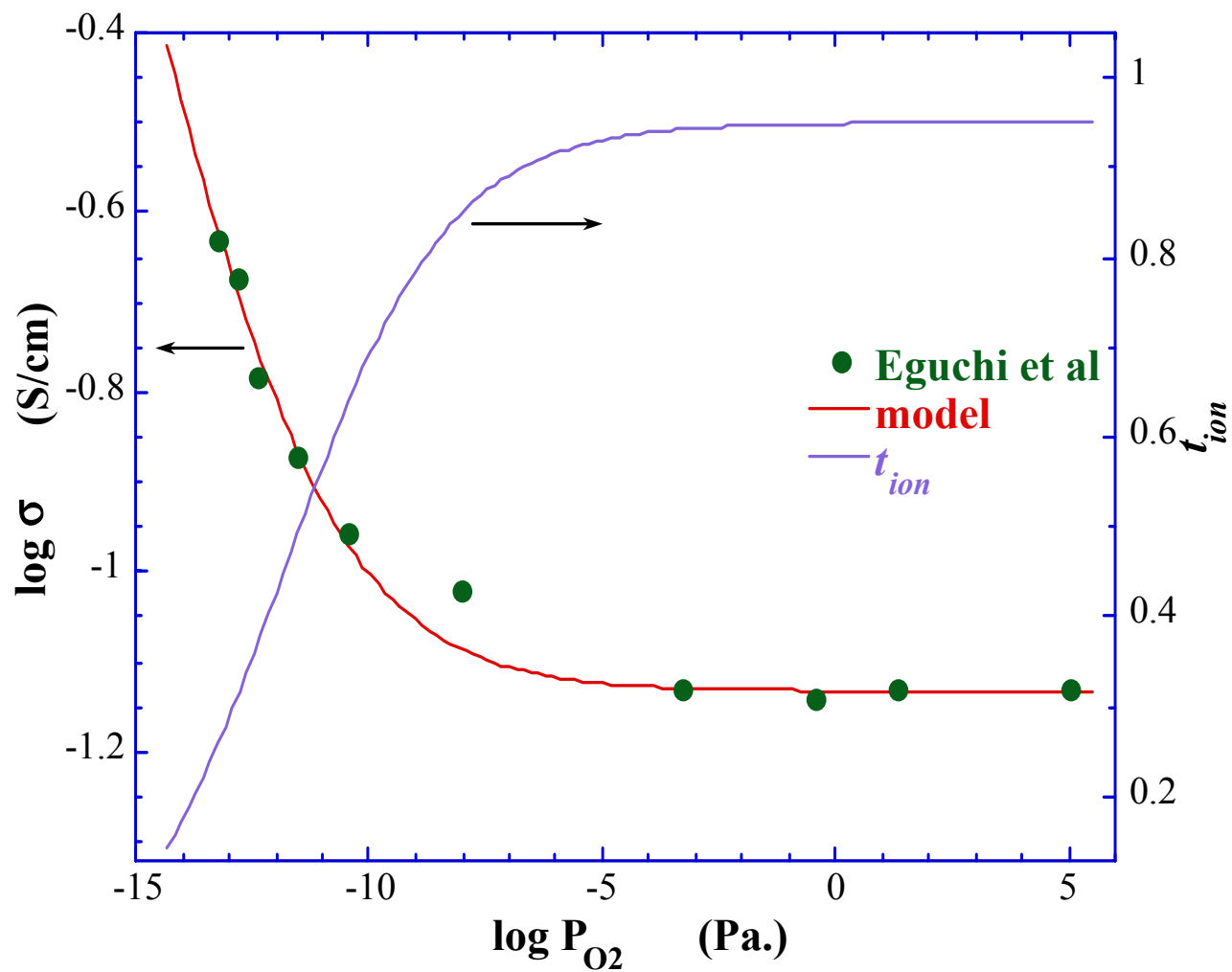


COMPARISON OF DEFECT MODEL WITH NUMERICAL SOLUTION TO DEFECT EQUATIONS FOR $\text{Ce}_{0.8}\text{Sm}_{0.2}\text{O}_{1.9-\delta}$



* O. Porat and H. L. Tuller, *J. Electroceramics* 1 (1997) 42.

FIT OF DEFECT MODEL TO CONDUCTIVITY DATA*



* Eguchi et al, *Solid State Ionics* **52** (1992) 265.

FUNDAMENTAL EQNS. & DEFNS.

Nernst-Planck

$$j_i = -D_i \nabla c_i - u_i c_i \nabla \phi$$

Current

$$J = \sum_i J_i = q \sum_i z_i j_i$$

Average conductivity

$$\bar{\sigma}_i^{-1} = L^{-1} \int_0^L [\sigma_i(x)]^{-1} \cdot dx$$

Charge neutrality

$$\sum_i z_i c_i = z_V c_V + z_A c_A + z_e c_e \approx 0$$

Local equilibrium

$$\phi_L - \phi_0 = \Delta\phi = \Phi_{ext} - \Phi_{th} - k_B T (z_V q)^{-1} \ln(c_{V_L} / c_{V_0})$$

j	flux
J	current
c	concentration
ϕ	potential
z	charge num.
q	elec. charge
s	conductivity
u	mobility
D	diffusivity
L	thickness
k_B	Boltz. const.
Φ_{th}	Nernst poten.
Φ_{ext}	exter. potential
T	temperature

Subscripts

V	O_2 vacancies
e	electrons

LINEAR POTENTIAL MODEL

For $\nabla j_i = 0$,

$$\nabla c_V \approx 0$$

and/or

$$D_e \gg D_V$$

Defect distribution

$$c_i(x) = \frac{c_{iL} - c_{i0} \exp(\beta\Delta\phi) + (c_{i0} - c_{iL}) \exp(\beta\Delta\phi x/L)}{1 - \exp(\beta\Delta\phi)}$$

Defect flux $j_i(\Delta\phi) = \frac{J_i(\Delta\phi)}{z_i q} = -u_i \frac{\Delta\phi}{L} \cdot \frac{c_{iL} - c_{i0} \exp(\beta\Delta\phi)}{1 - \exp(\beta\Delta\phi)}$

$$\beta = \frac{z_V D_V - z_e D_e}{D_e - D_V} \cdot \frac{q}{k_B T}$$

typically

$$\beta \sim \frac{q}{k_B T}$$

Current efficiency

$$\zeta_J(\Delta\phi) = \frac{J(\Delta\phi)}{J_V(\Delta\phi)} = 1 + \frac{J_e(\Delta\phi)}{J_V(\Delta\phi)}$$

Power efficiency

$$\zeta_P(\Delta\phi) = \frac{J(\Delta\phi)}{J_V(\Delta\phi)} \cdot \frac{\Phi_{ext}}{\Phi_{th}}$$

Transference number $\bar{t}_{ion}(\Delta\phi) = \left[1 + \frac{J_e(\Delta\phi)}{J_V(\Delta\phi)} \cdot \frac{\ln(c_{V0}/c_{VL}) + \beta\Delta\phi}{\ln(c_{e0}/c_{eL}) + \beta\Delta\phi} \right]^{-1}$

NON-LINEAR POTENTIAL MODEL

$$\nabla^2 \phi = \lambda \nabla^2 c_V \quad \leftarrow \nabla J = 0 \text{ \& \; } \nabla j_i = 0$$

$$\gamma = \frac{\phi_L - \phi_0}{\lambda L} - \frac{c_{V_L} - c_{V_0}}{L}$$

$$\lambda = \frac{(z_V - z_e)k_B T}{z_e q c_A}$$

$$z_V = 2, \quad z_e = z_A = -1$$

$$c_V(x) - c_{V_0} - (\phi(x) - \phi_0)/\lambda = -\gamma x \dots \dots \dots \text{(A)}$$

(Nernst-Planck + current equation)

$$(z_V u_e j_V - u_V j_e) c_V - j_V u_e c_A = \frac{q D_e D_V}{k_B T} (6 c_V - c_A) \nabla c_V$$

$$c_V(x) - c_{V_0} - \frac{(D_V \gamma - j_V) c_A}{6 D_V \gamma} \cdot \ln \frac{6 D_V \gamma c_V(x) - j_V c_A}{6 D_V \gamma c_{V_0} - j_V c_A} = -\gamma x \dots \dots \dots \text{(B)}$$

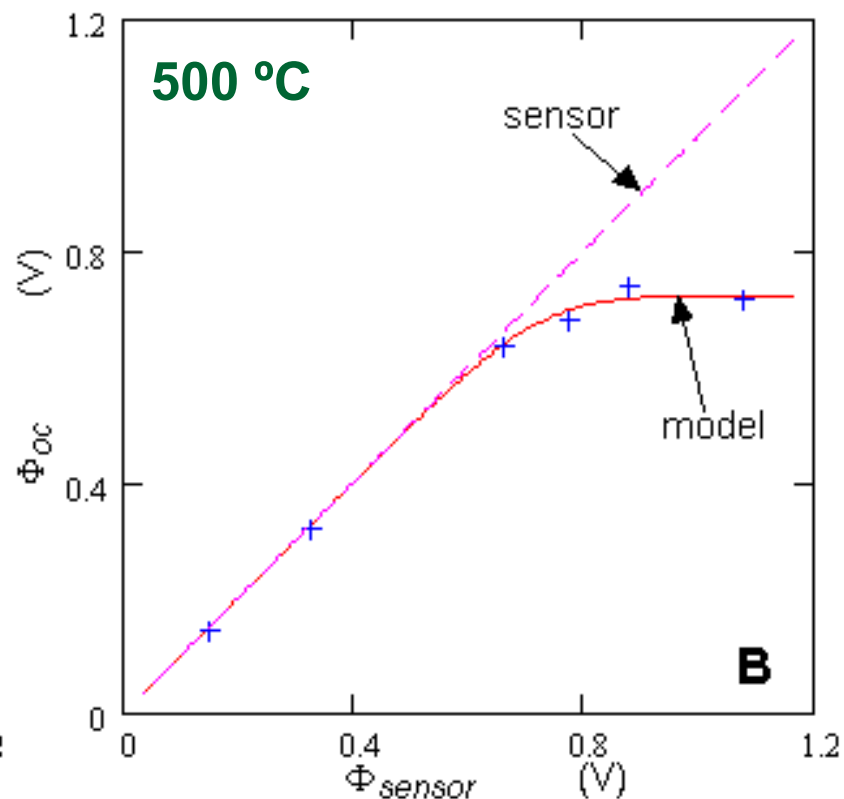
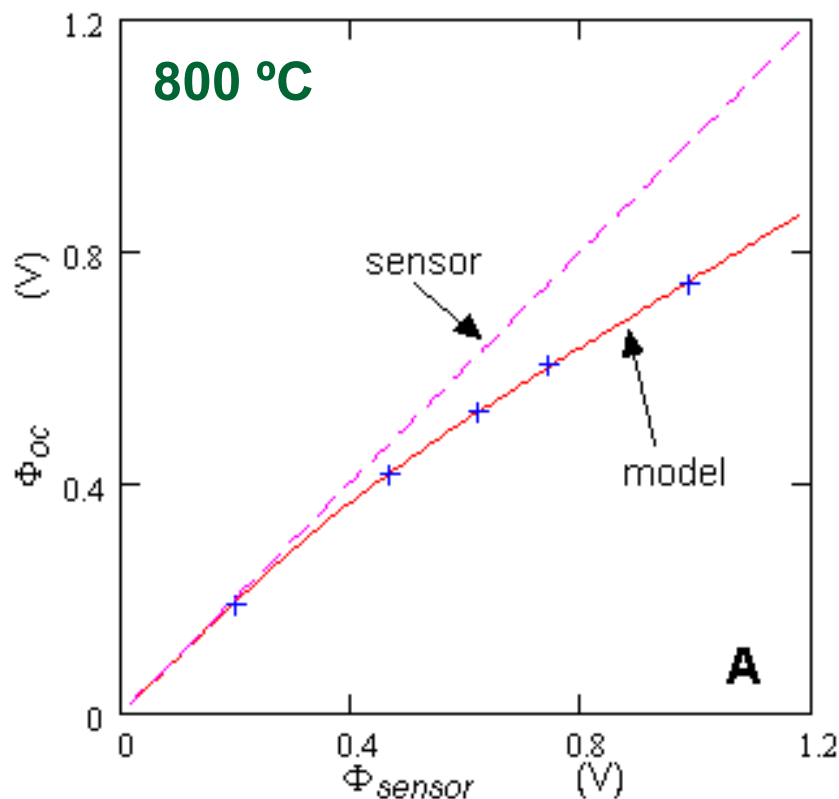
(A) - (B)

$$\phi(x) = \phi_0 - \frac{(D_V \gamma - j_V) k_B T}{z_V q D_V \gamma} \cdot \ln \frac{6 D_V \gamma c_V(x) - j_V c_A}{6 D_V \gamma c_{V_0} - j_V c_A}$$

$$\gamma = -k_B T \frac{z_V u_e j_V - u_V j_e}{6 q D_e D_V}$$

OPEN CIRCUIT (Φ_{oc}) vs. NERNST (Φ_{sensor}) POTENTIAL FOR SDC SOFC

model (—), expt. data (+), sensor (---)



H₂/H₂O (CO/CO₂), Pt/ SDC / Pt, Air

Modeling the Relationship between Thickness ratio, Performance and ESB Decomposition Potential

$$J_V^{SDC} = J_V^{ESB}$$

+

$$\phi_L - \phi_0 = \Delta\phi = -\frac{(z_V q D_V \gamma - J_V) k_B T}{z_V^2 q^2 D_V \gamma} \cdot \ln \frac{z_V^2 (z_V - z_{e,h}) q D_V \gamma c_{V_L} - J_V c_A}{z_V^2 (z_V - z_{e,h}) q D_V \gamma c_{V_0} - J_V c_A}$$

$$\gamma = \lambda^{-1} \Delta\phi / L - (c_{V_L} - c_{V_0}) / L = -\frac{z_{e,h} D_{e,h} J_V + z_V D_V J_{e,h}}{z_V (z_V - z_{e,h}) q D_{e,h} D_V}$$

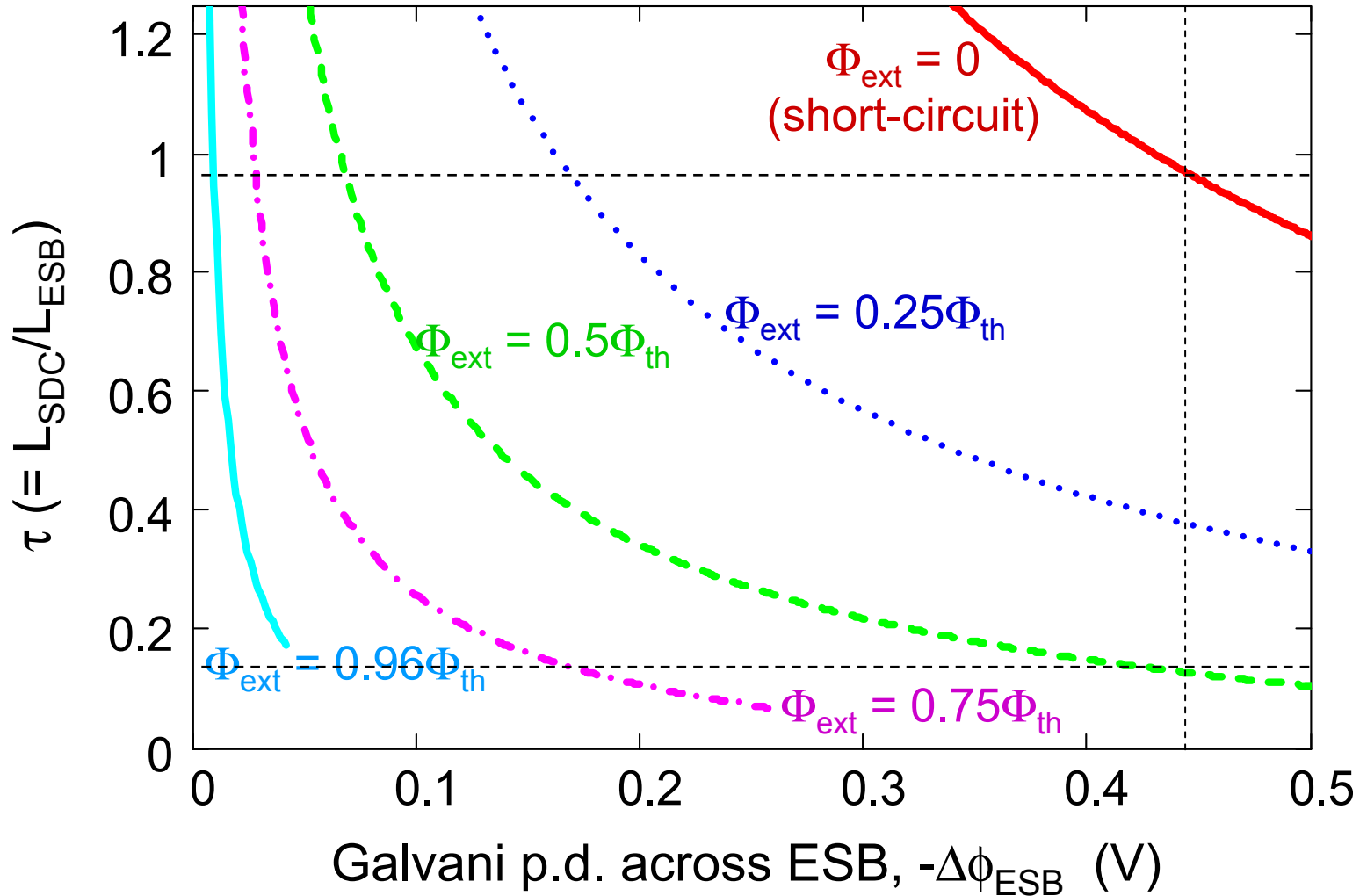
$$\tau_{oc} = \frac{L^\varepsilon}{L^\delta} = \frac{D_e^\varepsilon D_V^\varepsilon \left[\frac{3(c_{V_L}^\varepsilon - c_{V_0}^\varepsilon)}{-D_e^\varepsilon - 2D_V^\varepsilon} - \frac{(D_e^\varepsilon - D_V^\varepsilon)c_A^\varepsilon}{(-D_e^\varepsilon - 2D_V^\varepsilon)^2} \ln \frac{2(-D_e^\varepsilon - 2D_V^\varepsilon)c_{V_L}^\varepsilon + D_e^\varepsilon c_A^\varepsilon}{2(-D_e^\varepsilon - 2D_V^\varepsilon)c_{V_0}^\varepsilon + D_e^\varepsilon c_A^\varepsilon} \right]}{D_h^\delta D_V^\delta \left[\frac{c_{V_L}^\delta - c_{V_0}^\delta}{D_h^\delta - 2D_V^\delta} + \frac{(D_h^\delta - D_V^\delta)c_A^\delta}{(D_h^\delta - 2D_V^\delta)^2} \ln \frac{2(D_h^\delta - 2D_V^\delta)c_{V_L}^\delta - D_h^\delta c_A^\delta}{2(D_h^\delta - 2D_V^\delta)c_{V_0}^\delta - D_h^\delta c_A^\delta} \right]}$$

$$\varepsilon = \text{SDC}, \quad \delta = \text{ESB}$$

$$\tau = \frac{\frac{q(\Phi_{ext} - \Phi_{th})}{k_B T} - \frac{1}{2} \ln \frac{c_{V_L}}{c_{V_0}} - \frac{q\Delta\phi^\delta}{k_B T} + 3 \left(\frac{c_{V_0}^\varepsilon}{c_A^\varepsilon} - \frac{1}{2} \right) \left[\left(\frac{c_{V_L}}{c_{V_0}} \right)^{-\frac{1}{2}} \exp \left(\frac{q(\Phi_{ext} - \Phi_{th} - \Delta\phi^\delta)}{k_B T} \right) - 1 \right]}{\frac{D_V^\delta}{D_V^\varepsilon} \cdot \frac{c_A^\delta}{c_A^\varepsilon} \cdot \left\{ \frac{q\Delta\phi^\delta}{k_B T} - \left(\frac{c_{V_L}^\delta}{c_A^\delta} + \frac{1}{2} \right) \left[1 - \exp \left(\frac{q\Delta\phi^\delta}{k_B T} \right) \right] \right\}}$$

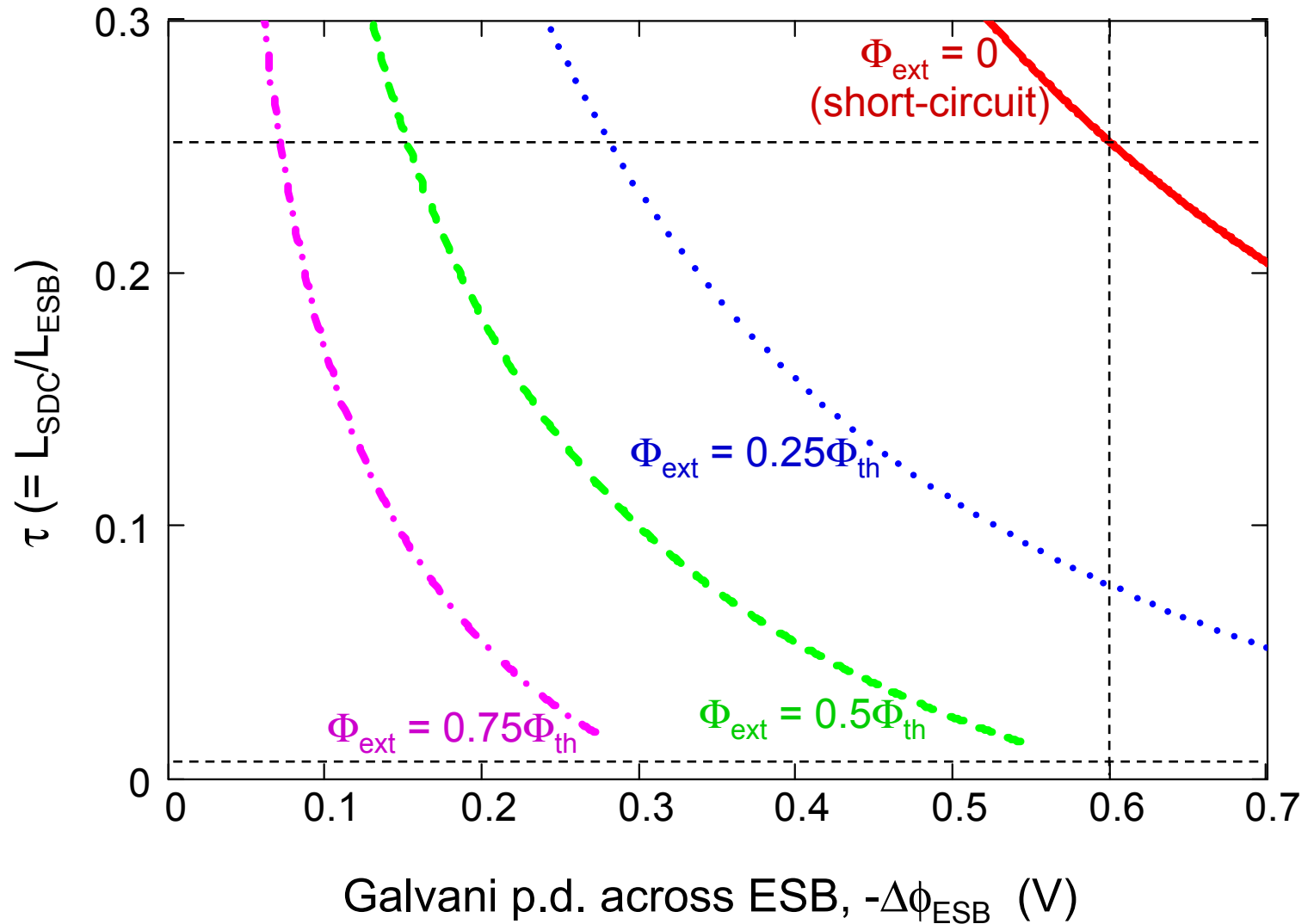
ELECTROLYTE DESIGN

Determination of thickness ratio at 800 °C



ELECTROLYTE DESIGN

Determination of thickness ratio at 500 °C



RELATIVE THICKNESS (τ) PREDICTED BY MODEL

		τ	$1/\tau = L_{\text{ESB}}/L_{\text{SDC}}$	ASR* (Ωcm^2)
800 °C	short circuit	0.98	1.0	0.010
	max. power	0.14	7.1	0.003
500 °C	short circuit	0.25	4.0	0.11
	max. power	~0.007	~140	0.05

* $L = L_{\text{ESB}} + L_{\text{SDC}} = 10 \mu\text{m}$

SUMMARY

Developed Analytical Models for Transport in Oxides

- Based on Nernst-Planck flux equation and defect equilibria (minimal assumptions)
- Determined external equilibrium constant, K_R
- Verified transport model for SDC OCP vs. anode P_{O_2}
- Verified defect model for SDC conductivity vs. P_{O_2}
- Used model to predict SDC/ESB thickness ratio

@500 °C

$$140 > L_{ESB}/L_{SDC} > 4$$

$$0.05 \text{ } \Omega\text{cm}^2 < \text{ASR} < 0.11 \text{ } \Omega\text{cm}^2$$

SUMMARY-Continued

Fabricated and Tested ESB/SDC Bilayer Electrolytes

- Achieved OCP = 1.00 V and $t_i = 0.9$
- Demonstrated increasing relative thickness of ESB increases OCP and t_i

Consistent with bilayer concept

Consistent with computer model predictions

Fabricated thin ($\sim 10 \mu\text{m}$) anode supported GDC SOFCs

- Maximum power density @650 C = 270 mW/cm²

Developed New Bismuth Oxide Electrolyte (DWSB)

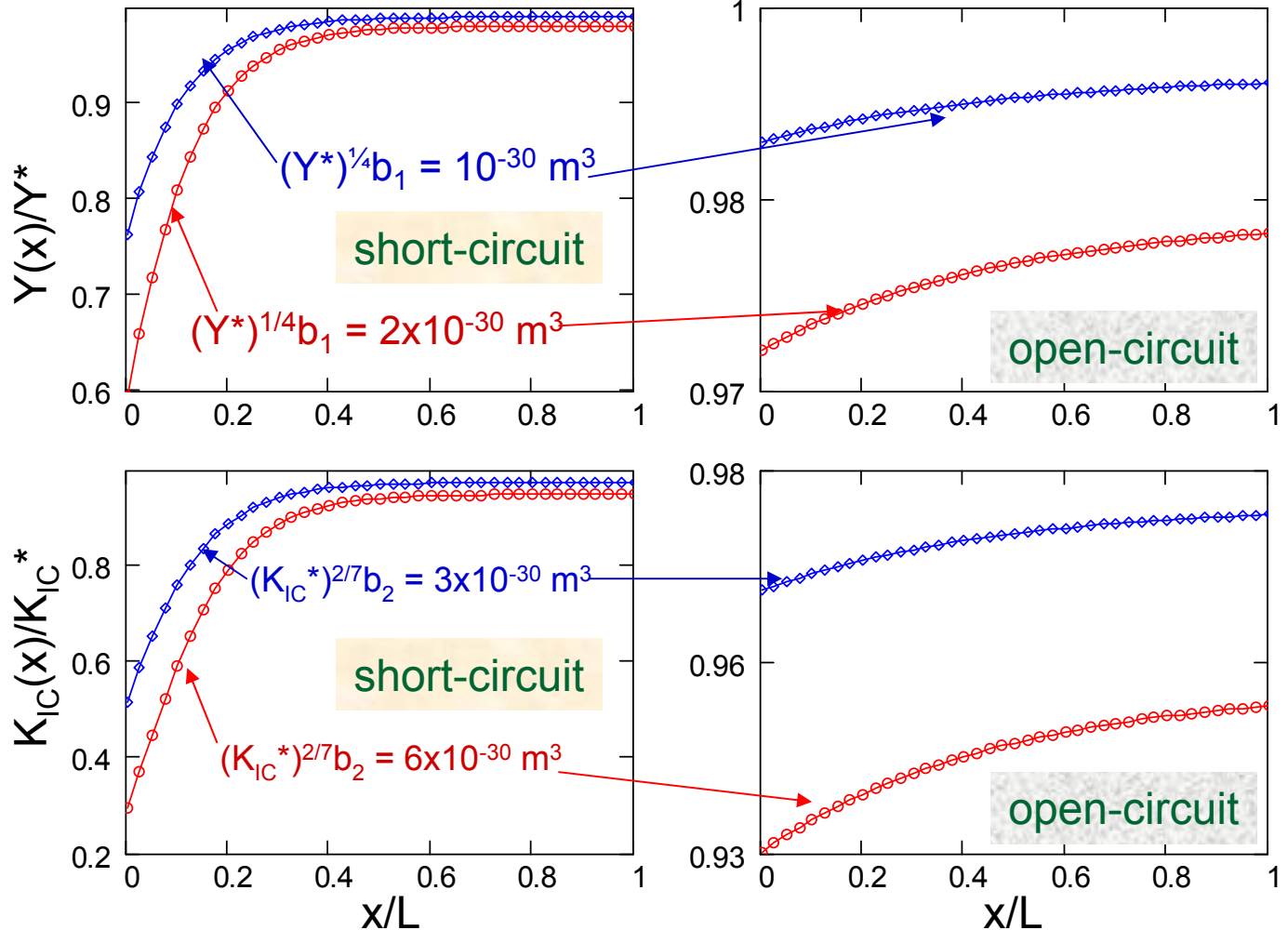
- Highest conductivity of any known electrolyte
 - 0.57 S/cm at 800°C
 - 0.043 S/cm at 500°C

APPLICABILITY TO SOFC COMMERCIALIZATION

$$Y(x) = Y^* [(Y^*)^{1/4} b_1 c_V(x) + 1]^{-4}$$

$$K_{IC}(x) = K_{IC}^* [(K_{IC}^*)^{2/7} b_2 c_V(x) + 1]^{-3.5}$$

**SPATIAL
VARIATION OF
ELASTIC
MODULUS (Y)
& FRACTURE
TOUGHNESS
(K_{IC}) IN SOFC
ELECTROLYTES**



Activities for the Next 3 Months...

Develop cathode compatible with Bi_2O_3 electrolyte.

Fabricate and test thin anode-supported ESB/GDC SOFCs.